Sources of phase noise in homodyne and heterodyne phase modulation devices used for tissue oximetry studies

N. Ramanujam, C. Du, H. Y. Ma, and B. Chance
Department of Biochemistry and Biophysics, University of Pennsylvania, Philadelphia, Pennsylvania 19104

(Received 30 December 1997; accepted for publication 13 May 1998)

The objective of this study was to characterize sources of phase noise in homodyne and heterodyne phase modulation devices (PMDs) used for tissue oximetry measurements. Each PMD incorporates a laser diode modulated at a radio frequency in the 50–200 MHz range, an optical detector and a homodyne/heterodyne phase sensitive detector. The intensity modulated light which propagates through tissue is attenuated and undergoes a phase shift, which reflects the mean time of flight of the photons through the tissue. The measured amplitude and phase can be used to determine hemoglobin saturation in tissues using equations based on diffusion theory. Four studies were performed to characterize the sources of phase noise. First, the signal to noise ratio was characterized to determine if the PMDs are operating at the shot noise or detector noise limit. Second, the accuracy of the three PMDs for measuring phase shifts in tissue were compared by using them to measure the phase shift as a function of path length change in air, at a constant amplitude, and at signal to noise ratios comparable to that measured from tissue. The third source of noise measured was the phase shift that results from optical attenuation of the signal (phase-amplitude cross talk) at a constant path length, to characterize intensity dependent phase shifts in the PMDs. Finally, the interchannel interference of a dual wavelength PMD which uses radio frequency multiplexing to perform phase measurements at two wavelengths simultaneously was compared to that of a dual wavelength PMD which uses time multiplexing to perform phase measurements at two wavelengths serially to determine the effect of each on phase error. © *1998 American Institute of Physics.* [S0034-6748(98)01308-2]

I. INTRODUCTION

In the near-infrared (NIR) spectral region, the number of light scattering events in tissue is approximately two orders of magnitude greater than the number of absorption events. This allows light to penetrate several centimeters into the medium before being absorbed or emitted through boundaries, therefore enabling sampling of large tissue volumes, such as the breast, brain, and skeletal muscle. Endogenous chromophores include oxy and deoxy hemoglobin/myoglobin, cytochrome oxidase, and water.[1] The absorption of light by these chromophores can be used to determine important physiological indicators such as hemoglobin/myoglobin oxygenation,[2] blood volume changes,[3,4] and respiration.[5] Tissue scattering is associated with microscopic variations in the tissue dielectric constant and is affected by the concentration of mitochondria in cells,[6] cell size, and volume fraction, and alterations in refractive indices of both intracellular and extracellular compartments due to chemical modulators, such as carbohydrates.[7,8] Quantification of the absorption and scattering properties of tissue can enable the quantification of important physiological markers.

Photon migration in tissue is a diffusion process in which discrete photons are either elastically scattered or totally absorbed according to linear absorption and scattering coefficients. These coefficients can be quantitatively described using a model of light propagation based on the diffusion approximation to the radiative transfer theory, which is valid at distances from the light source much larger than the mean free path of light scattering.[9] Although physicochemical descriptions of tissue scattering coefficients are empirical, the absorption coefficient can be described as a function of the product of the extinction coefficient and concentration of the chromophore; if more than one chromophore is present, the absorption coefficient is the sum of the absorption coefficients of contributing chromophores.[10]

The diffusion approximation can be used to calculate the absorption and scattering coefficients of tissue using frequency domain measurements of diffusely reflected light.[11,12] A typical frequency domain apparatus incorporates a laser source with its intensity modulated at the megahertz frequency range using a radio frequency (rf) oscillator and an optical detector coupled to a phase sensitive detector. The intensity modulated light which propagates through tissue is attenuated and undergoes a phase shift. The phase shift of the detected signal reflects the mean time of flight of the photons propagating through the tissue (5–10 ns) and the amplitude of the signal reflects the attenuation characteristics of the medium. Tissue absorption and scattering can be determined from the amplitude and phase using the diffusion equation.[13,14]

Our objective is to compare the sources of phase noise in three types of frequency domain apparatuses (differing mainly by the method of phase detection employed by each), which we will refer to here as phase modulation devices (PMDs). These PMDs are specifically designed to measure and quantify hemoglobin saturation (percentage of hemoglo-

TABLE I. Characteristics of the of the 140 (1), 200 (2), and 50.1 (3) MHz phase modulation devices (PMDs).

PMD	Radio frequency (MHz)	Laser diode (nm)	Modulation (%)	Laser power (mW)	Delivered laser power (μW)	Optical detector	Frequency at optical detector (MHz)	Phase detector	Frequency at phase detector (MHz)
1	140	786	90	10	20	APD	140	In phase and	140
Hom		830		30	40	R928, T08	140	quadrature	140
2	200	754	90	5	10	R928	0.054	Zero crossing	0.054
Het		816		5	10		0.023		0.023
3	50.1	786	90	10	20	T08	50.1	Zero crossing	0.10
Het									

bin that is oxygenated) in tissues, at wavelengths between 750 and 850 nm, where oxygenated/deoxygenated hemoglobin are the primary absorbers. Typically, tissue hemoglobin concentrations range from 0 to 100 μM and the clinically relevant PO_2 range is between 20 and 50 mm Hg.[15] Sevick *et al.*[15] have used time domain spectroscopy to measure photon path lengths as a function of PO_2 of a solution containing 27 μM hemoglobin, 0.5% intralipid, and 0.01% yeast added to consume oxygen (scattering coefficient: $\mu_s' = 7.25\ \mathrm{cm}^{-1}$). The results indicate that as the PO_2 is increased from 20 to 60 mm Hg, the path length change is 1 cm at 754 nm and 0.25 cm at 816 nm. If a PMD modulated at 200 MHz is used to make these measurements, the path length changes would correspond to a phase shift of 3.25° at 754 nm and 0.8° at 816 nm, assuming that the velocity of light in tissue is approximately 22 cm/ns.[15] These small phase shifts suggest that sources of noise in phase measurements need to be characterized and minimized for hemoglobin saturation quantification.

Four studies were performed to characterize the sources of phase noise in the three PMDs. First, the signal to noise ratio was characterized to determine if the PMDs are operating at the shot noise or detector noise limit. Second, the accuracy of the three PMDs for measuring phase shifts in tissue were compared by using them to measure the phase shift as a function of path length change in air (theoretical value can be obtained from the velocity of light in air), at a constant amplitude and at signal to noise ratios comparable to that measured from tissue. The third source of noise measured was the phase shift that results from optical attenuation of the signal (phase-amplitude cross talk) at a constant path length, to characterize intensity dependent phase shifts in the PMDs. The final objective was to compare the interchannel interference of a dual wavelength PMD which uses frequency multiplexing to perform phase measurements at two wavelengths simultaneously to that of a dual wavelength PMD which employs time multiplexing to perform phase measurements at two wavelengths serially to determine the effect of each on phase measurements. These studies follow and expand on the work of several groups who have performed studies to quantify the performance of frequency domain instrumentation.[16–18] In particular, Fantini *et al.*[16] have done a series of systematic tests to quantify the precision and accuracy of phase and amplitude measurements using their frequency domain spectrometer for the optical characterization of biological tissues. Yokoyomo *et al.*[17] and Pogue *et al.*[18] have shown previously in phase-amplitude cross-talk tests that optical detectors including both avalanche photodiodes (APDs) and photomultiplier tubes (PMTs) used in PMDs can cause an intensity dependent phase shift in the modulated signal transiting the optical detector.

II. INSTRUMENTATION

Table I summarizes the characteristics of the three PMDs. The 140 MHz PMD (1) is a homodyne unit which employs in-phase and quadrature (I&Q) circuitry for phase detection of the optical signal modulated at the rf, whereas the 50.1 MHz PMD (3) employs heterodyning in a mixer at the output its optical detector to convert the optical signal modulated at the rf into an audio frequency range prior to phase detection with a zero crossing detector. The 200 MHz PMD (2) also employs heterodyning but by the injection of a rf signal at a slightly offset frequency (required to produce the heterodyne signal) at the second dynode stage of its PMT prior to phase detection with a zero crossing detector.

Laser diodes have been employed as these light sources can be modulated at high frequencies (up to 300 MHz) with modulations approaching 100%. The wavelengths selected coincide with the absorption bands of oxygenated and deoxygenated hemoglobin in the NIR window as these PMDs are primarily used for tissue oximetry studies. The laser powers range from 5 to 30 mW, and the laser power delivered to the tissue ranges from 10 to 40 μW.

Three optical detectors were evaluated. The R928 PMT (Hamamatsu, R928) has an extended red response. However, the frequency response of this PMT declines at around 50 MHz. The T08 PMT (Hamamatsu, R5600-01) has a parallel dynode structure which provides a better frequency response up to 400 MHz. However, its cathode has a decreased quantum efficiency above 810 nm. Avalanche photodiodes (APDs) (Hamamatsu, C5331, operating voltage: 5 V, gain setting: 4.5×10^4 V/W, temperature stability: $\pm$2.5% between 15 and 35 °C) have a larger bandwidth (up to 1 GHz) than R928 and T08 PMTs and have built in amplifiers which provide output signals within the range of low gain PMTs. However, the APD has a 0.25 mm^2 aperture which decreases optical coupling efficiency.

(i) 140 MHz PMD: Figure 1 shows a schematic of the dual wavelength 140 MHz PMD. A 140 MHz rf oscillator (Wilmanco, VS-A-140.0, 13 dBM) is used to sinusoidally modulate two laser diodes operating at 786 and 830 nm (Sharp Laser Diodes, LT031MD, 10 mW; LT024MD, 10 mW), respectively, using a 10 Hz electromechanical switch.

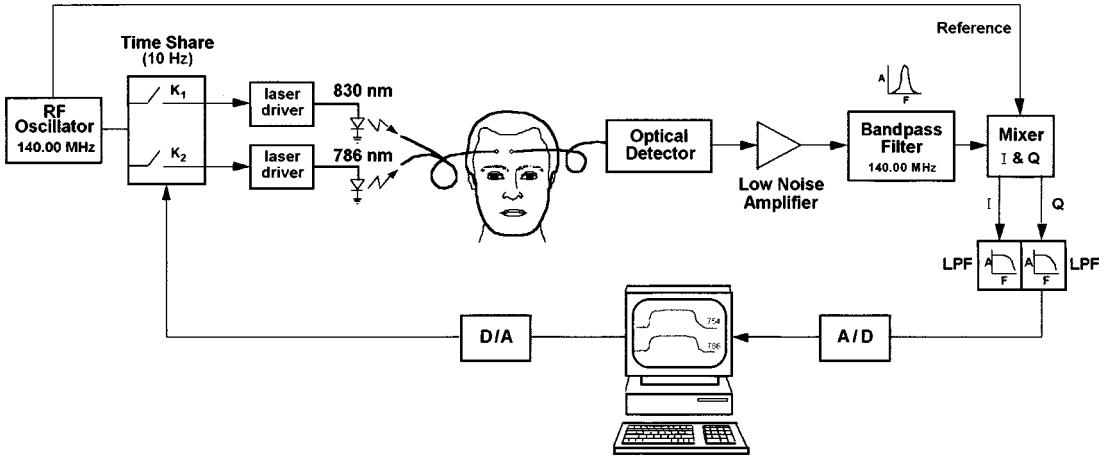

FIG. 1. 140 MHz phase modulation device.

The intensity modulated light is delivered to the tissue from both laser diodes using a bifurcated fiber-optic bundle. The phase shifted and attenuated optical signal from the sample is delivered via a second fiber-optic bundle to the optical detector (the 140 MHz PMD was evaluated using all three optical detectors described previously).

The output of the optical detector is amplified (Hamamatsu, C5594-22, 36 dB gain), filtered and then delivered to an I&Q demodulator (Mini-Circuit, MIQY-140D). The 140 MHz oscillator also provides a reference signal through the use of a 50/50 power splitter to the I&Q demodulator. The dc outputs of the I&Q demodulator, *I* and *Q*, which are the cosine and sine components of the phase and amplitude are filtered using a low pass filter with a 10 Hz band width and then digitized by an analog to digital converter (Real Time Devices, 2210). The phase and amplitude are then calculated by computer software. The details of I&Q demodulation are described in detail elsewhere.[19]

(ii) 200 MHz PMD: A schematic of the 200 MHz PMD is illustrated in Fig. 2. Laser diodes at wavelengths of 754 and 816 nm are sinusoidally modulated by two constructed rf oscillators (14 dBM) operating at 200.054 and 200.023 MHz, respectively. The phase shifted and attenuated optical signals from the sample are delivered to an R928 PMT. A reference signal at 200 MHz generated by a third constructed rf oscillator (14 dBM) is coupled to the second dynode stage of the PMT through a resonant circuit of 10 kΩ impedance to provide heterodyne mixing with the signals at 200.054 and 200.023 MHz with 50% modulation. The resulting signals at a frequency of 54 kHz at 754 nm and 23 kHz at 816 nm are coupled to a constructed amplifier (20 dB gain) and separated using appropriate bandpass filters centered at 55 and 25 kHz, respectively. The phase shift of these signals is measured by a zero crossing pulse that triggers a sawtooth wave form which is terminated by the reference pulse provided by the mixing of the 200 MHz rf signal with those at 200.054

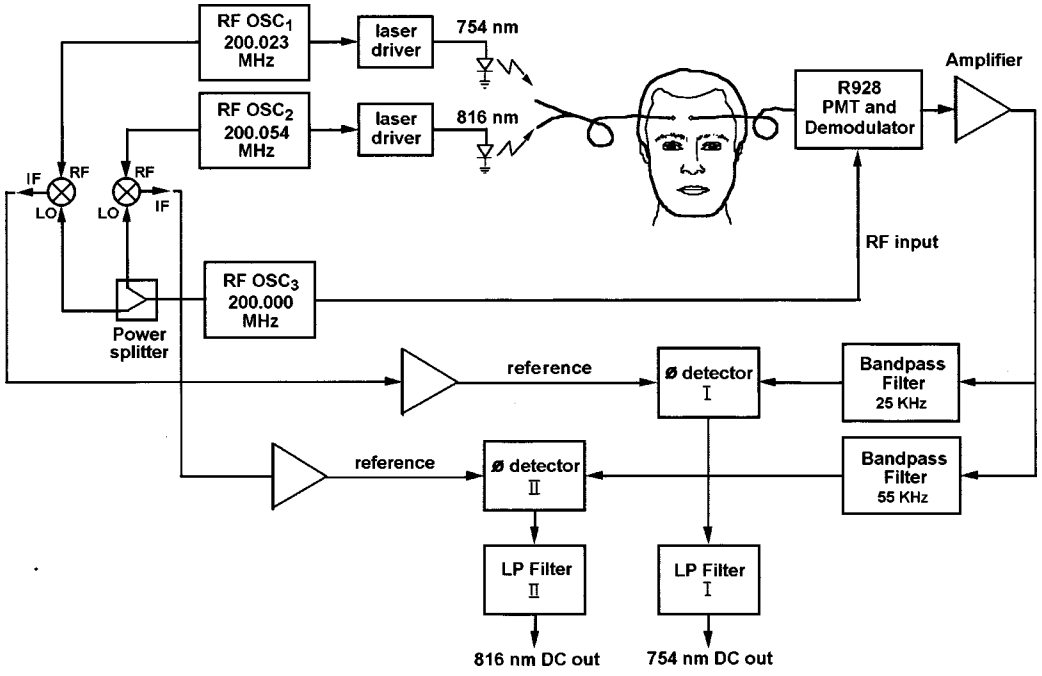

FIG. 2. 200 MHz phase modulation device.

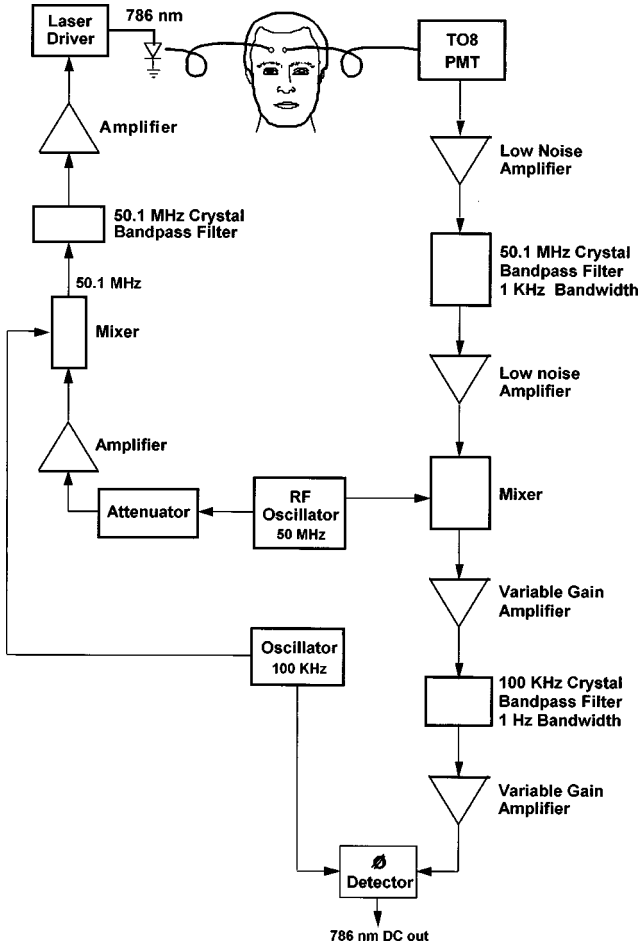

FIG. 3. 50.1 MHz phase modulation device.

and 200.023 MHz, respectively. Output voltages representing the phase and amplitude at both frequencies measured in a 30 Hz bandwidth are plotted on a strip chart recorder.

(iii) 50.1 MHz PMD: Figure 3 shows a schematic of the 50.1 MHz PMD. The output signals from a 50 MHz rf oscillator (Texas Instruments, 2N3904) and a 100 kHz oscillator (Texas, Instruments, MC1350) are mixed in an SBL-diode mixer to produce the 50.1 MHz rf signal. The output of the mixer passes through a 50.1 MHz filter which eliminates the lower side bands and is amplified by a second amplifier (Texas Instruments, NE592). A 786 nm wavelength laser diode (Sharp Laser Diodes, LT031MD, 10 mW) is sinusoidally modulated by the rf signal (12 dBM) at 50.1 MHz. The phase-shifted and attenuated optical signal is delivered to a T08 PMT. The output of the PMT is coupled to two low noise amplifiers (Mini-Circuits, MAN1LN, 30 dB gain) with a 50.1 MHz bandpass filter with a 1 kHz bandwidth, between them to ensure that there is no noise loading of the second amplifier. The 50.1 MHz signal is combined in a mixer with a reference signal from the 50 MHz rf oscillator to produce a signal at 100 kHz. This output is further amplified by two amplifiers (Texas Instruments, NE592), with a 100 kHz, 1 Hz bandwidth filter between them. The phase shift of the output signal is measured using a zero-crossing phase detector (Krohn–Hite, 6220B) with respect to a reference signal from the 100 kHz oscillator. Output voltages representing the phase and amplitude measured in a 1 Hz bandwidth are plotted on a strip chart recorder.

III. EXPERIMENTAL METHODS

A simple optical apparatus was used to test the performance of the three PMDs described above. The optical apparatus consists of two plano convex lenses: the first lens (focal length: 7.5 cm, diameter: 5 cm) serves to collimate the illumination from the fiber-optic bundle (diameter: 1 cm, numerical aperture: 0.55) which is coupled to the modulated laser diode; the second lens focuses the collimated beam onto a second fiber-optic bundle (focal length: 7.5 cm, diameter: 5 cm) which is coupled directly to the optical detector used in the PMD. Neutral density filters of O.D., 0.1, 0.3, 0.5, and 1.0 were used for the purpose of attenuating the optical signals in a calibrated manner during the various experimental studies.

(i) Signal to noise ratio: The first goal was to characterize the relationship between the signal and noise measured at the output of the optical detector(s) used in each of the three PMDs. The signal and corresponding noise were measured over a wide signal range in the optical detector. The signal incident on the optical detector was incrementally changed by uniformly attenuating the optical signal in the collimated region between the two lenses by neutral density filters of O.D., 0.1, 0.3, 0.5, and 1.0. The corresponding signal and noise at the output of the optical detector were measured using a spectrum analyzer (Hewlett Packard, 8554B) at a fixed bandwidth before and after the addition of each neutral density filter.

The signal to noise ratio (SNR) was calculated according to the following equation:

$$\mathrm{SNR}=\frac{S_{\mathrm{ac}}-N_{\mathrm{ac}}}{N_{\mathrm{ac}}}, \tag{1}$$

where, S_{ac} is the photocurrent corresponding to the ac signal and N_{ac} is the photocurrent corresponding to the ac noise measured at the output of the optical detector.

(ii) Phase shift as a function of path length change in air: The accuracy of each PMD for performing phase measurements was characterized by using it to measure the velocity of light in air. The following equation relates the phase shift measured per unit path length change in air to the velocity of light:

$$\Delta\phi=2\pi F\,\frac{\Delta L}{c} \quad \text{or} \quad \frac{\Delta\phi}{\Delta L}=2\pi F\,\frac{1}{c} \tag{2}$$

where, $\Delta\phi$ is the phase shift in radians, F is the frequency of the modulated laser source, c is the velocity of light in air which is $2.9979E+10$ cm/s and ΔL is the path length change in air.

Each PMD was used to measure the phase shift as a function of path length change in air using the optical apparatus. The path length change in air was achieved by changing the distance between the two lenses of the optical apparatus from an initial separation of 3 cm to a final separation of 7 cm in 1 cm increments. Increasing the separation where the beam is collimated ensured that at each path length po-

sition, the amplitude loss was negligible. This was done to eliminate any intensity dependent phase shifts. The phase shift and signal to noise ratio was measured at each path length position. The experimental phase shift as a function of path length change in air was fit to a linear function, the slope of which was compared to the theoretical phase shift per unit length change in air calculated using Eq. (2).

The phase shift per unit path length change in air was measured over a range of signal to noise ratios which was achieved by attenuating the signal incident on the optical detector using neutral density filters. When a PMT was used, the phase shift as a function path length change in air was also measured as a function of several high voltages. Furthermore, the phase shift per unit path length change in air was compared between different types of optical detectors used with the same PMD in order to make a direct comparison between them.

Finally, in order to compare the phase measurement accuracy of the three PMDs and corresponding optical detectors at a signal to noise ratio that is comparable to measurements made from biological tissues, the three PMDs were used to measure the signal from the forehead of a human volunteer at several source and detector separations ranging from 2 to 5 cm. The phase measurement accuracy of the three PMDs was determined by evaluating the error in their measurement of phase shift per unit path length change in air at a signal to noise ratio similar to that obtained from the forehead of the volunteer at a source and detector separation of 3 cm. The signal to noise ratio obtained from this measurement was considered to be representative of typical signal to noise ratios measured from tissues, *in vivo*.

(iii) Phase shift as a function of amplitude attenuation with and without dynode feedback: Each PMD and corresponding optical detector was used to measure phase shift as a function of amplitude attenuation using the optical apparatus. The signal incident on the optical detector was incrementally attenuated using neutral density filters of O.D. 0.1, 0.3, 0.5, and 1 between the two plano convex lenses. The path length between the two lenses in the collimated part of the beam was maintained at a constant separation of 3 cm. During the experiment, the phase shift, amplitude, and signal to noise ratio were measured before and after the addition of each neutral density filter. When a PMT was used, the data were measured as a function of several high voltages. Furthermore, the phase shift as a function of amplitude attenuation was measured using a single PMD with different optical detectors of the same type as well as with the three different types of optical detectors.

A dynode feedback loop which regulates the dynode voltages to produce a predetermined constant signal output level in the PMT[12] was incorporated into the 200 MHz PMD to test the feasibility of using this technique to overcome the phase shift due to amplitude attenuation in the optical detector. Dynode feedback has the advantage that (1) the amplifier and phase detector are supplied with a constant signal input and thus have a minimal contribution to drift or phase shift and (2) although, there is a change in the transit time delay with a change in the dynode voltage of the PMT, this is a reproducible quantity that depends on the physical characteristics of electron multiplication. The 200 MHz PMD with dynode feedback was used to measure the phase shift as a function of amplitude attenuation using the optical apparatus. The phase shift, the corresponding high voltage, and the signal to noise ratio were measured before and after the addition of each neutral density filter. The phase shift measured as a function of high voltage using dynode feedback was compared to the phase shift due to amplitude loss at a fixed high voltage over the same optical attenuation range, using the 200 MHz PMD.

(iv) Interchannel interference of dual wavelength PMDs which employ frequency multiplexing versus time multiplexing: The final objective was to compare the interchannel interference of a dual wavelength PMD which uses frequency multiplexing to perform optical measurements at two wavelengths simultaneously versus a dual wavelength PMD which employs time multiplexing to perform optical measurements at two wavelengths serially.

The first goal was to characterize the harmonics and intermodulation products of the heterodyned frequency encoded signals at both wavelengths and evaluate their effect on interchannel interference in the 200 MHz PMD. Using a spectrum analyzer, three specific experiments were performed (at a high voltage of 740): (1) only the modulated laser source at 754 nm was turned on; the frequency spectrum of the corresponding dynode demodulated signal at 54 kHz was evaluated at the output of the 55 kHz bandpass filter as well as at the output of the 23 kHz bandpass filter (to test the leakage), (2) the previous experiment was repeated with only the modulated laser source at 816 nm turned on, and (3) both modulated laser sources were turned and the frequency spectrum from both the 55 and 23 kHz bandpass filters were measured.

Next, the interchannel interference of these harmonics and intermodulation products was evaluated on the measurement of phase shift as a function of path length change in air. With both modulated laser sources on, the optical signal from both sources was appropriately attenuated such that the signal in the optical detector due to both sources was equivalent. The phase shift as a function of path length change in air was measured at both wavelengths simultaneously as described previously, at a high voltage of 740. This experiment was repeated at different signal to noise ratios by changing the signal incident on the optical detector.

The final goal was to evaluate the interchannel interference of the harmonics and intermodulation products on the measurement of phase shift as a function of amplitude attenuation. The amplitude-phase relationship discussed previously is the resulting phase shift due to an amplitude loss of the optical signal at the same wavelength (primary wavelength). In the presence of interchannel interference, there will be an additional contribution to the phase shift due to amplitude losses of the optical signal at the other wavelength (secondary wavelength). To test this hypothesis, a fiber bundle from the primary wavelength source was coupled directly to one leg of a bifurcated fiber-optic bundle, the common end of which is connected to the PMT. An optical fiber bundle from the secondary wavelength source was coupled through the collimated optical apparatus described previ-

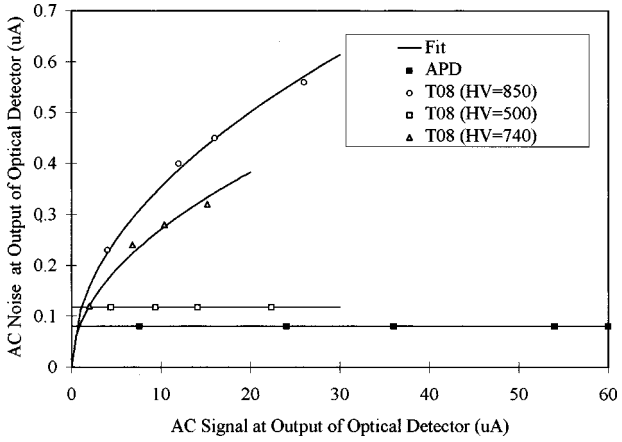

FIG. 4. Experimental data and corresponding fits of the noise as a function of ac signal measured at the output of the T08 PMT and APD optical detectors used in conjunction with the 140 MHz APD at 786 nm (HV is high voltage). A bandwidth of 2.5 kHz was used to reduce the effect of $1/f$ noise.

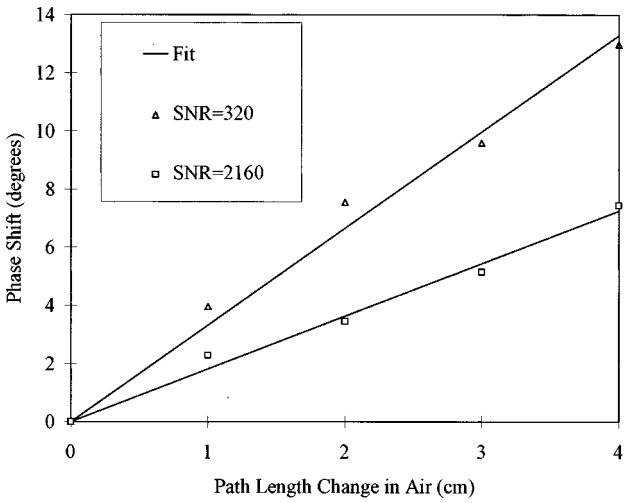

FIG. 5. Experimental data and corresponding linear fits of the phase shift as a function of path length change in air measured at high and low signal to noise ratio (bandwidth is 10 Hz) using the 140 MHz PMD and APD at 786 nm.

ously to the second leg of the bifurcated fiber-optic bundle. Initially, the optical signals from both laser sources were appropriately attenuated such that the signal incident on the optical detector from both sources was equivalent. Then by keeping the signal at the primary wavelength constant, the optical signal from the secondary wavelength source was incrementally changed by placing neutral density filters of O.D. 0.1, 0.3, 0.5, and 1.0 in the collimated part of the beam. The phase and amplitude at both wavelengths were measured at the output of the 25 and 55 kHz bandpass filters at each attenuation step.

To compare time multiplexing to frequency multiplexing, an experiment was done to characterize (1) the phase shift as a function of path length change in air and (2) the phase shift as a function of amplitude attenuation using the dual wavelength 140 MHz PMD with the APD which uses an electromechanical switch to alternate between the two wavelength sources. The results obtained from this study were compared to analogous results obtained from the frequency encoded 200 MHz PMD, to compare the interchannel interference effects of each.

IV. RESULTS

(i) Signal to noise characteristics: Figure 4 displays experimental data and corresponding fits of the ac noise as a function of the ac signal measured at the output of the T08 PMT and APD used in conjunction with the 140 MHz PMD at 786 nm (a bandwidth of 2.5 kHz was used to reduce the effect of $1/f$ noise). Figure 4 indicates that at a high voltage of 740 and 850 of the PMT, the noise is related to the square root of the ac signal which is reflected by the functional form of the fits. Therefore, the quantum fluctuations in the detected light impose an ultimate limit on the signal to noise ratio. However, when the T08 PMT is used at a high voltage of 500 or when an APD is used, the noise is independent of the ac signal, indicating that the signal to noise ratio is detector noise limited. Similar experiments performed with the R928 PMT demonstrated that the signal to noise ratio is shot noise limited at high voltages greater than 640. Figure 4 demonstrates that there is an excellent agreement between the experimental data and corresponding fits; this is representative of fits to similar experimental data obtained with the other PMDs and corresponding optical detectors.

(ii) Phase shift as a function of path length change in air: The phase shift as a function of path length change in air was measured with all three PMDs and corresponding optical detectors. Figure 5 shows the experimental data and corresponding linear fits of the phase shift versus path length change in air measured at a high and low signal to noise ratio (10 Hz bandwidth) using the 140 MHz PMD and APD at 786 nm. Figure 5 shows that there is good agreement between the experimental data and the corresponding fits. These are typical of fits to similar experimental data obtained with the other PMDs and corresponding optical detectors. Note that a small degradation of the fit is observed at the lower signal to noise ratio in Fig. 5. This can be explained by the fact that as the signal to noise ratio decreases, the uncertainty in the phase shift as a function of path length change increases hence resulting in a poorer fit to the theoretical model.

Figure 6 displays the phase shift per unit path length in air $(\Delta\varphi/\Delta L)$ measured as a function of signal to noise ratio (10 Hz bandwidth) using the 140 MHz PMD and APD at 786 nm. The solid line represent the theoretical value of $\Delta\varphi/\Delta L$, calculated from Eq. (2) and the dotted lines represent an incremental error of 10% relative to the theoretical value. The experimental $\Delta\varphi/\Delta L$ was extracted from the slope of the linear fit to the experimental data. Figure 6 illustrates that the error in $\Delta\varphi/\Delta L$ increases as the signal to noise ratio decreases reflecting the inverse relationship between these two parameters.

Figures 7(a)–7(c) display the signal to noise ratio as a function of source-detector separation on the forehead of a human volunteer measured with the three PMDs. The signal to noise ratio was calculated from the ac signal and noise measured at the output of the optical detector (2.5 kHz bandwidth). Figure 7(a) compares the signal to noise ratio measured as a function of source-detector separation using three different optical detectors with the 140 MHz PMD at 786

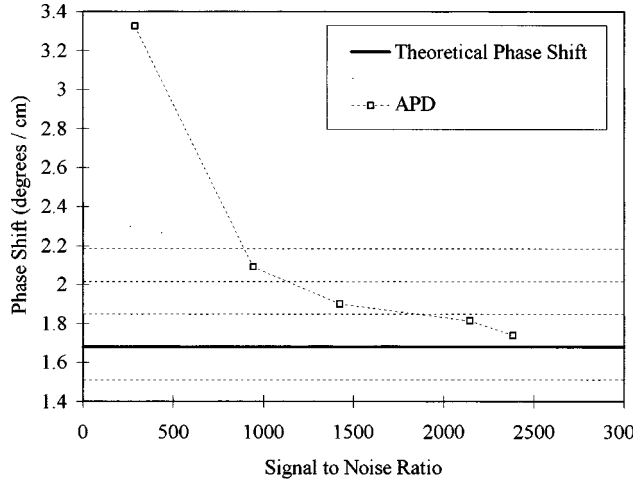

FIG. 6. Phase shift per unit path length change in air measured as a function of signal to noise ratio (bandwidth is 10 Hz) using the 140 MHz PMD and APD at 786 nm.

nm. Note that both the APD and R928 PMT display a signal to noise ratio ranging from 10 to 1 as the source-detector separation increases from 2.5 to 3.5 cm. The T08 PMT has a signal to noise ratio that is more than twice that of the APD and R928 PMT at a similar source-detector separation.

Figure 7(b) displays the signal to noise ratio as a function of source-detector separation measured with the 200 MHz PMD and R928 PMT at 754 nm. The signal to noise ratio ranges from 40 to 20 for a source-detector separation ranging from 2.5 to 3.5 cm. A comparison of the 200 MHz PMD to the 140 MHz PMD used with the same R928 PMT indicates that for a source-detector separation of 3 cm for example, the latter PMD has approximately a factor of four lower signal to noise ratio. This may be attributed to the fact that the signal loss in the R928 PMT is more significant due to the higher modulation frequency of the signal.

Figure 7(c) displays the signal to noise ratio as a function of source-detector separation for the 50.1 MHz PMD and T08 PMT at 786 nm. For a source-detector separation ranging from 2.5 to 3.5 cm, the signal to noise ratio ranges from 70 to 10 (at a high voltage of 850). Note that the signal to noise ratio at a particular source and detector separation is highly dependent on the gain of the PMT. A comparison of this PMD to the 140 MHz PMD used with the T08 PMT indicates that for a source-detector separation of 3 cm, the latter PMD has a factor of two lower signal to noise ratio (at a high voltage of 850). Again, this is attributed to the increased losses in the R928 PMT at the higher modulation frequency of 140 MHz.

Table II provides the accuracy of the three PMDs for measuring $\Delta\varphi/\Delta L$ in air at signal to noise ratios that are similar to that measured from the forehead of a human volunteer at a source-detector separation of 3 cm. Signal to noise ratios have been recalculated in a 1 Hz bandwidth for the purpose of comparison between the different PMDs and corresponding optical detectors. Evaluation of all three PMDs and corresponding optical detectors indicate that the error in $\Delta\varphi/\Delta L$ increases as the high voltage increases. A comparison between the three optical detectors used with the

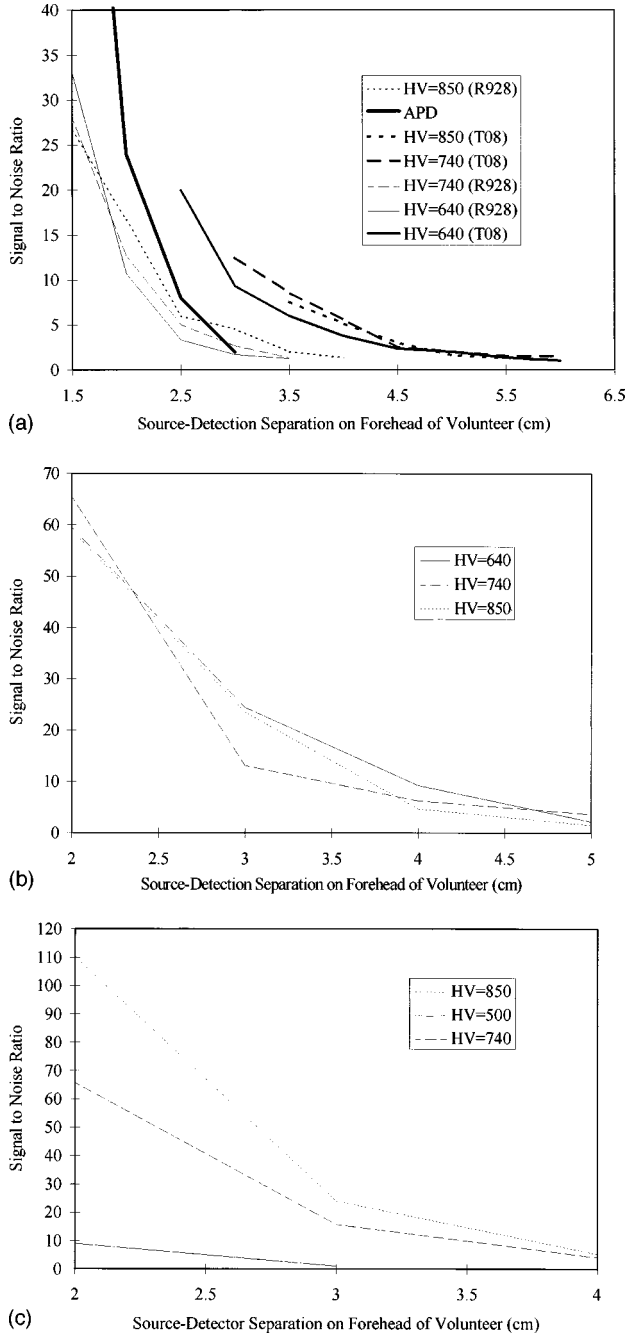

FIG. 7. Signal to noise ratio as a function of source and detector separation on the forehead of a human volunteer using (a) the 140 MHz PMD with all three optical detectors, (b) 200 MHz PMD with the R928 PMT and (c) 50.1 MHz PMD with the T08 PMT. The signal to noise ratios were measured at the output of the optical detectors using a bandwidth of 2.5 kHz.

140 MHz PMD indicates that the APD has the lowest phase measurement accuracy while the R928 PMT demonstrates the highest. A comparison between the 200 MHz PMD with the R928 PMT (at a high voltage of 640) and the 140 MHz PMD with the R928 PMT (at a high voltage of 740) indicates that the latter PMD has approximately a factor of two increase in phase error. A comparison between the 50.1 MHz PMD with the T08 PMT (at a high voltage of 740) and the 140 MHz PMD with the T08 PMT (at a high voltage of 740) indicates that the latter PMD has approximately a factor of three increase in phase error. Note that the 200 MHz PMD

TABLE II. The accuracy of the three phase modulation devices (PMDs) for measuring phase shift per unit path length change in air (ϕ/L) at SNR (recalculated in a 1 Hz bandwidth) comparable to measurements from the forehead of a human volunteer at a source and detector separation of 3 cm.

PMD	Optical detector	High voltage (V)	SNR	Measured ϕ/L (°/cm)	Error in ϕ/L (°/cm)	Error in ϕ/L (%)
140 MHz PMD (786 nm)	APD	N/A	50	3.2	1.52	90
	R928	740	125	1.4	0.2	12
		850	250	1.2	0.4	23
	T08	740	550	1.23	0.36	21
		850	600	0.62	1	60
200 MHz PMD (754 nm)	R928	640	1250	2.32	0.08	3.33
		740	750	2.22	0.18	7.50
		850	1250	2.714	0.314	13
50.1 MHz PMD (786 nm)	T08	500	50	SNR too low	···	···
		740	750	0.55	0.05	8
		850	1250	0.56	0.04	6.67

and the 50.1 MHz PMD demonstrate comparable phase measurement accuracies at equivalent high voltages. The basis for the superior performance of these two PMDs relative to the 140 MHz PMD is the superior signal to noise ratio of these systems under similar experimental constraints.

(iii) Phase shift as a function of amplitude attenuation, in the absence of a path length change: The phase shift due to amplitude attenuation was measured and characterized using the three PMDs and corresponding optical detectors. Figure 8 displays the experimental data measured using the 200 MHz PMD and R928 PMT at 754 nm, at a high voltage of 640 and bandwidth of 30 Hz. The data were fit to the following function:

$$\Delta\phi = \frac{k}{I}, \tag{3}$$

where, I is the ac photocurrent at the output of the optical detector and k is the free parameter of the fit, which in this case was 2.3. Note that a constant value of 1 was added to the experimental phase data for fitting purposes, since the initial phase was zero after base line subtraction. Evaluation of Fig. 8 indicates that the phase shift varies inversely with the ac signal in the optical detector as reflected by the functional form of the fit. Figure 8 demonstrates that there is good agreement between the experimental data and corresponding fit and this is representative of fits to experimental data obtained with the other PMDs and optical detectors.

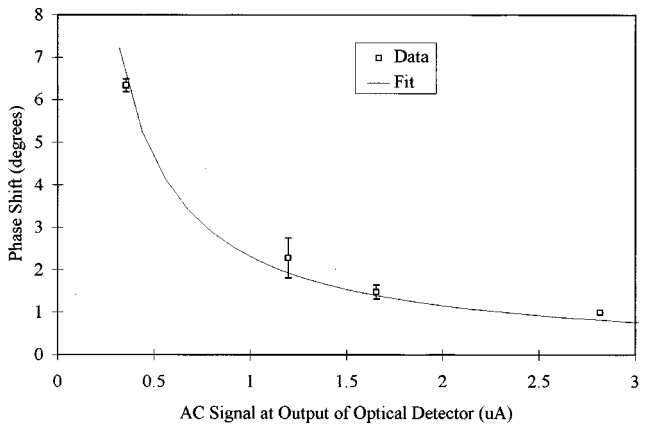

FIG. 8. Experimental data and corresponding fit of the phase shift measured as a function of amplitude attenuation (achieved with a series of neutral density filters of O.D. 0.1, 0.3, 0.5, and 1.0 with resulting corresponding signal to noise ratios of 450, 350, 280, and 100, respectively) at a high voltage of 640 V (bandwidth is 30 Hz).

In order to compare the phase shift due to amplitude attenuation between the different PMDs, the phase shift was measured over a 1.0 O.D. attenuation range using each PMD and corresponding optical detector(s). A singular value of phase shift per unit amplitude attenuation was determined by subtracting the phase shift measured at a 1 O.D. attenuation from the phase shift measured in the absence of attenuation, with each PMD. Although the phase shift is not linearly related to attenuation represented in O.D., denoting the phase shift per amplitude attenuation in these units allows for a comparison to be made between the different PMDs, since this is the common denominator in all the measurements.

Table III compares the phase shift per unit amplitude attenuation ($\Delta\varphi/M$) of the three PMDs and corresponding optical detectors. Evaluation of $\Delta\varphi/M$ in the 200 MHz PMD with the R928 PMT indicates that it is approximately 4.5°/O.D. and decreases slightly with increasing high voltage when the photocurrent in the PMT in the absence of attenuation is the same at all three high voltages. A comparison of $\Delta\varphi/M$ measured using the three different optical detectors with the 140 MHz PMD indicates that $\Delta\varphi/M$ of the APD is comparable to that of the R928 PMTs at similar signal to noise ratios, which is in the range of 10–20°/O.D. However, a comparison of $\Delta\varphi/M$ of the T08 PMT to that of both the APD and R928 PMT at similar signal to noise ratios indicates that it is almost an order of magnitude lower at all three high voltages. Evaluation of the T08 PMT when used with the 50.1 MHz PMD indicates that its $\Delta\varphi/M$ is an order of magnitude higher than when it is used in conjunction with the 140 MHz PMD. Furthermore, it is also higher than that of the other optical detectors used with their corresponding PMDs. It is speculated that the large phase shifts observed

TABLE III. A summary of the phase shift per unit amplitude attenuation (ϕ/M) measured with all the three phase modulation devices (PMDs) and corresponding optical detectors. I_0 represents the ac signal in the optical detector in the absence of calibrated attenuation (using neutral density filters) and SNR represents the corresponding signal to noise ratio recalculated in a 1 Hz band width.

PMD	Optical detector	High voltage (V)	I_0 (μA)	SNR	ϕ/M (°/O.D.)
200 MHz PMD (754 nm)	R928 (1)	640	3.7	2600	5.34
		740	3.5	1900	4.5
		850	3.3	1350	3.5
140 MHz PMD (786 nm)	APD	*N/A*	60	7450	9.718
	R928(1)	500	16	13300	17.27
		740	32	7950	11.002
		850	64	5650	9.626
	R928(2)	500	23	290	16.17
		740	40	100	12.23
	T08(1)	500	27	230	1.982
		740	18	50	1.06
		850	32	50	0.95
	T08(2)	740	55	140	2.41
		850	36	45	1.834
50.1 MHz PMD (786 nm)	T08(1)	500	36	300	31.3
		740	42	75	35.7
		850	48	60	40.3

here may be attributed to additional phase shifts through the rf electronics in the 50.1 MHz PMD.

Finally, a comparison was made between two different optical detectors of the same type, used with the same PMD to determine what the variability in $\Delta\varphi/M$ is. The two R928 PMTs (1) and (2) used with the 140 MHz PMD indicate that for a similar signal level in the PMT (in the absence of attenuation) and at the same high voltage, the $\Delta\varphi/Ms$ of both optical detectors are similar to within 10%. A comparison between the two T08 PMTs (1) and (2) used with the 140 MHz PMD indicates that the phase shift due to PMT (1) is a factor of two greater than that due to PMT (2) at a similar signal level in the PMT and at the same high voltage of 850.

The results in Table III indicate that the phase shift as a function of amplitude attenuation is significant in all three optical detectors used with their corresponding PMDs. Furthermore, the phase shift is inversely related to the ac signal in the optical detector suggesting that a linear relationship cannot be used to describe the relationship between phase shift and amplitude attenuation. Finally, the relationship between phase shift and attenuation is a function of the gain in the optical detector. Although in principle, a look up table of phase error corrections can be developed to rectify this problem, the dependence of phase shift on both photocurrent and gain makes this difficult to implement. An alternate solution is to use the principle of dynode feedback to maintain a constant signal output from the optical detector such that intensity dependent phase shifts are eliminated.

Dynode feedback was incorporated into the 200 MHz PMD to regulate the high voltage such that a constant signal was maintained at the output of the PMT.[12] The phase shift as a function of high voltage change (amplitude attenuation) was then measured over a 1.0 O.D. range of amplitude attenuation and is shown in Fig. 9. Figure 9 indicates that there is a linear relationship between phase shift and high voltage. This phase shift is due to the transit time delay in the PMT which is a function of the high voltage and is approximately 0.2°/V.

Figure 10 compares the phase shift measured as a function of amplitude attenuation represented in O.D. (a) in the presence of dynode feedback and (b) in the absence of dynode feedback at a fixed high voltage (640 V), using the 200 MHz PMD. Note that the signal to noise ratio range over which the signal is attenuated for both measurements is identical (signal to noise ranges from 450 to 100, measured in a 30 Hz bandwidth). Evaluation of Fig. 10 indicates that the phase shift due to amplitude attenuation and hence, high voltage change has a linear relationship with O.D., but the phase shift due to amplitude attenuation at a fixed high voltage has a nonlinear relationship with O.D. Furthermore, the nonlinearity varies as a function of high voltage. Although the phase shift as a function of a change in the high voltage is significant, it can be characterized by just one simple linear function that relates phase shift to high voltage over the

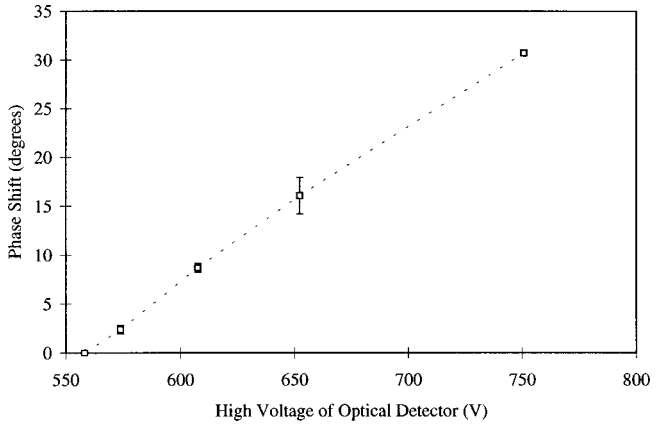

FIG. 9. Phase shift measured as a function of high voltage using the 200 MHz PMD with dynode feedback.

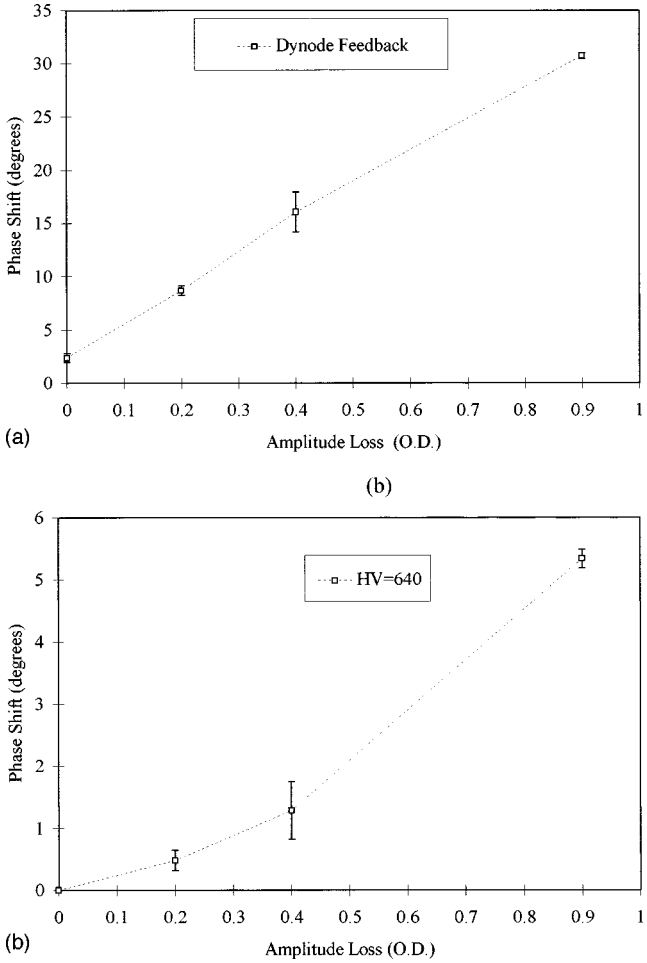

FIG. 10. Phase shift as a function of amplitude attenuation measured (a) with dynode feedback and (b) at a fixed high voltage, using the 200 MHz PMD and R928 PMT. The signal to noise ratio ranges from 450 to 100 (30 Hz bandwidth) for both measurements.

range that is typically used during measurements from biologic media.

(iv) Interchannel interference of dual wavelength PMDs with frequency and time multiplexing: Dual wavelength PMD with frequency multiplexing: Figure 11 displays the fast Fourier transform (FFT) of the heterodyne (dynode demodulated) signals from the 200 MHz PMD corresponding to the wavelengths at (a)-(b) 754 nm (the 816 nm laser diode is turned off) and (c)–(d) 816 nm (the 754 nm laser diode is turned off). Figure 11(a) displays the fundamental frequency (54 kHz) and corresponding harmonics (which account for 51% of the signal) at 754 nm, measured at the output of the 55 bandpass kHz filter. Figure 11(b) displays the leakage of this signal through the 25 kHz bandpass filter and indicates that only a very small fraction of the fundamental frequency is detected. Figure 11(c) displays the fundamental frequency (23 kHz) and corresponding harmonics (which account for 53% of the signal) at 816 nm, measured from the output of the 25 kHz bandpass filter. Figure 11(d) displays the leakage of this signal through the 55 kHz bandpass filter. Approximately 20% of the fundamental frequency and 65% of its second harmonic leak through; 50% of the leakage is contributed by the second harmonic.

Figures 12(a) and 12(b) display the FFT of the heterodyne signal measured at the output of the 25 kHz and the 55 kHz bandpass filters, respectively, when both laser diodes are simultaneously on. The laser diodes were appropriately attenuated such that the signal in the optical detector had an equivalent contribution at both wavelengths. Figure 12(a) indicates that the leakage of the 54 kHz signal through the 25 kHz bandpass filter is negligible while Fig. 11(b) indicates that the leakage from the 23 kHz signal and harmonics through the 55 kHz bandpass filter accounts for almost 25% of the 54 kHz signal. Also, the output of the 55 kHz bandpass filter contains amplitudes at frequencies of 85 and 133 kHz which correspond to intermodulation products of the 23 and 54 kHz signals. In summary, the heterodyne signal at 754 nm has a significant contribution from (1) the fundamental frequency and harmonics of the heterodyne signal at 816 nm and (2) the intermodulation products of the 23 and 54 kHz signals.

The effect of interchannel interference on the measurement of the phase shift as a function of path length change in air ($\Delta\varphi/\Delta L$) was evaluated at 754 nm using the 200 MHz PMD (a high voltage of 740 V was used). Table IV displays $\Delta\varphi/\Delta L$ in air at different signal to noise ratios (30 Hz bandwidth) in the absence of (only the 754 nm laser diode is on) and presence of interchannel interference (754 and 816 nm laser diodes are on). The error in $\Delta\varphi/\Delta L$ is within 0.05° at a signal to noise ratio of 360 and increases to 0.15° at a signal to noise ratio of 90, in the absence of interchannel interference. In the presence of interchannel interference, the error in $\Delta\varphi/\Delta L$ is almost a factor of five higher at a signal to noise ratio of 360 and decreases to a factor of three at a signal to noise ratio of 90. Note, that at each signal to noise ratio, the signal output from the optical detector from both the 754 and 816 nm laser diodes was equivalent.

The effect of interchannel interference on the amplitude and phase shift of the 54 kHz signal (754 nm) as a function of amplitude attenuation of the 23 kHz signal (816 nm) was evaluated next (a high voltage of 740 V was used). Figures 13(a) and 13(b) illustrate the amplitude and phase shift at 754 nm, respectively, for amplitude attenuation at 816 nm. Amplitude attenuation at 816 nm was achieved using neutral density filters while the amplitude at 754 nm was maintained at a constant value. Note that there is an additional data point on each graph which indicates the amplitude and phase at 754 nm, when the 816 nm laser diode is turned off. Figure 13(a) indicates that an approximate 1.0 O.D. loss at 816 nm results in an amplitude loss of less than 0.02 O.D. at 754 nm. However, the phase shift at 754 nm due to an amplitude loss of approximately 1.0 O.D. at 816 nm [Fig. 13(b)] is more than 0.9°.

(v) 140 MHz dual wavelength PMD with time multiplexing: To test the advantage of time multiplexing over the use of frequency multiplexing in multiwavelength PMDs, experiments were performed using the 140 MHz PMD and APD to characterize (1) the phase shift as a function of path length change in air when both the 786 and 830 nm laser diodes are operated serially using an electromechanical switch and (2) the amplitude and phase shift at 786 nm as a function of amplitude attenuation at 830 nm. Note that time multiplexing is used to alternate the rf modulation of the

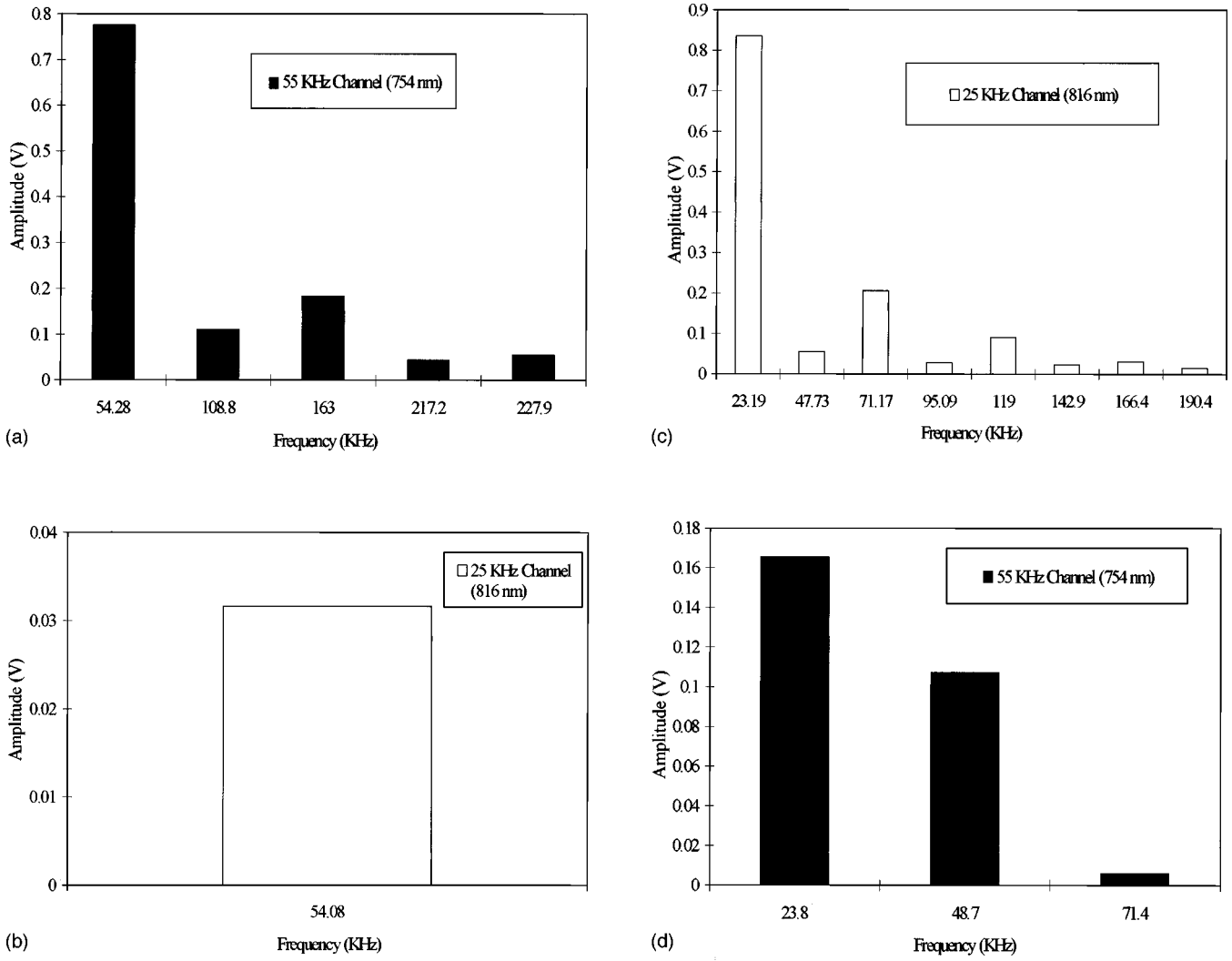

FIG. 11. (a)–(b) Fast Fourier transform (FFT) of the dynode demodulated signal at a frequency of 54 kHz (corresponding to the 754 nm wavelength laser source; the 816 nm wavelength laser source is turned off) measured from the output of the 55 and 25 kHz bandpass filters, respectively. (c)–(d) FFT of the dynode demodulated signal at a frequency of 23 kHz (corresponding to the 816 nm wavelength laser source; the 754 nm wavelength laser source is turned off) measured from the output of the 23 and 55 kHz bandpass filters, respectively.

laser diodes; hence the dc signal from the laser diodes is continuously on and does contribute to shot noise.

Table V displays $\Delta\varphi/\Delta L$ in air at different signal to noise ratios (10 Hz bandwidth) in the absence of interchannel interference (only the 786 nm laser diode is on) and the presence of interchannel interference (both the 786 and 830 nm laser diodes are on). In the absence of interchannel interference, the error in $\Delta\varphi/\Delta L$ is within 0.12° at a signal to noise ratio of 2120 and increases to 0.42° at a signal to noise ratio of 950. In the presence of interchannel interference, the error in $\Delta\varphi/\Delta L$ is a factor of two higher at a signal to noise ratio of 2120, and decreases to a factor of one and a half at a signal to noise ratio of 950.

Next, the amplitude and phase shift at 786 nm were measured as a function of amplitude attenuation at 830 nm using the 140 MHz PMD and APD. Figures 14(a) and 14(b) illustrate the amplitude and phase shift at 786 nm, respectively, for amplitude attenuation at 830 nm. Figure 14(a) indicates that the amplitude loss is less than 0.013 O.D. at 786 nm for an amplitude loss of approximately 0.8 O.D. at 830 nm. The phase shift at 786 nm is less than $\pm 0.3°$ over an amplitude increase of approximately 0.8 O.D. at 830 nm.

V. DISCUSSION

Application of PMDs for hemoglobin saturation quantification poses stringent requirements for accurately measuring phase shifts of intensity modulated light propagating through tissues. A signal to noise ratio characterization of the three PMDs indicates that for the case in which a PMT is used, shot noise imposes an ultimate limit at high voltages typically used for biological measurements. These results suggest that for the case in which the high gain PMT is used, the signal to noise ratio will increase only as the square root of the signal input. Since the FDA regulations on the intensity of laser light used in typical type I medical devices in the region of 650–900 nm is 20–100 μW,[12] the PMDs described here are operating close to the practical limits.

The phase shift as a function of path length change in air was measured using the three PMDs and compared at a sig-

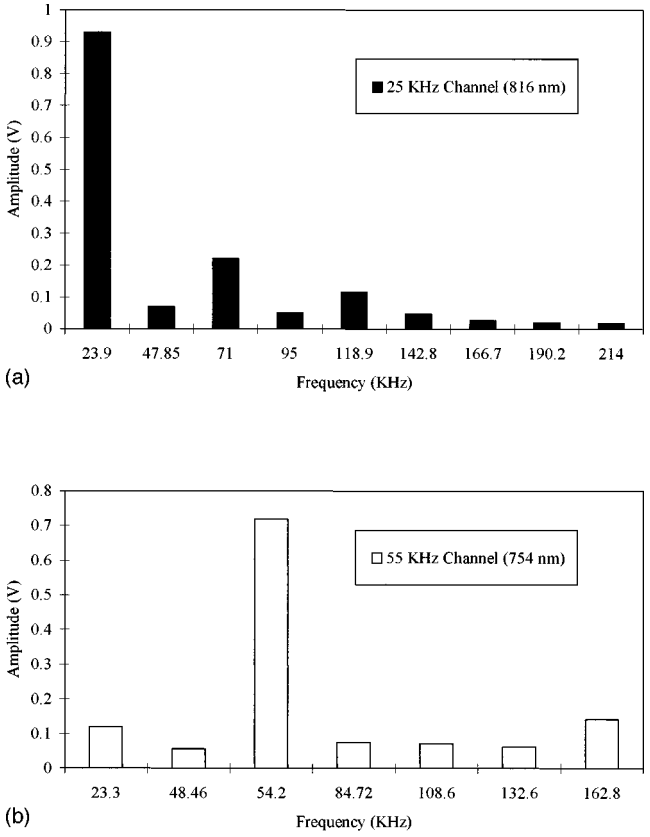

FIG. 12. Frequency spectrum measured from the output of (a) the 25 kHz and (b) the 55 kHz bandpass filters, respectively, with both wavelength sources simultaneously on. The laser diodes were appropriately attenuated such that the ac signal in the optical detector had an equivalent contribution from both wavelength sources.

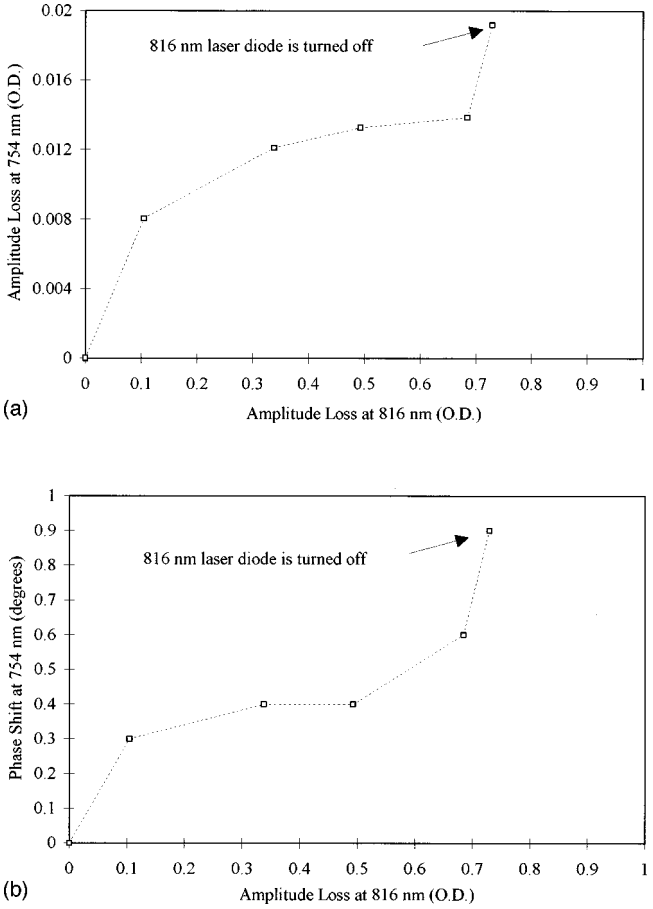

FIG. 13. (a) Amplitude loss of the 754 nm signal due to a 1.0 O.D. loss of the 816 nm wavelength source; (b) phase shift of the 754 nm signal due to a 1.0 O.D. amplitude loss of the 816 nm laser source. Measurements were made in a 30 Hz bandwidth.

nal to noise ratio comparable to measurements from the forehead of a human volunteer at a source and detector separation of 3 cm. A comparison of the 200 and 50.1 MHz heterodyne PMDs to the 140 MHz homodyne unit clearly indicates that heterodyning affords a superior phase measurement accuracy which is clearly a function of the signal to noise ratio. A comparison between the three optical detectors used with the 140 MHz PMD indicates that the APD has the lowest sensitivity while the T08 PMT has the highest sensitivity. However, the R928 PMT demonstrates the smallest phase measurement error at a comparable high voltage.

The phase shift due to amplitude attenuation is significant for all three PMDs and corresponding optical detectors. Yokoyama *et al.*[17] who have performed phase-amplitude cross-talk tests using the APD attribute intensity dependent phase shifts to the design limitations of the optical detector. In particular, the rise time of the APD which detects short width pulse light increases dramatically when the incident light intensity is decreased to a certain level.[20] Since such rise time changes are intrinsic in both APDs and PMTs (personal communication from Hamamatsu Photonics), the detector output phase exhibits an unwanted dependence on variations in the intensity of the incident light when detecting the modulated optical signal.

If uncorrected, phase shifts due to amplitude attenuation

TABLE IV. Measurement of phase shift as a function of path length change (ϕ/L) in air using the 200 MHz PMD and R928 PMT (high voltage is 740 V) at 754 nm when (a) only the 754 nm laser diode is turned on and (b) both the 754 and 816 nm laser diodes are turned on, at different signal to noise ratios (measurement bandwidth is 30 Hz). At each signal to noise ratio, the ac signal in the PMT from both laser diodes was equivalent.

Signal to noise ratio	(a) Measured ϕ/L(°/cm)	Error in ϕ/L(°/cm)	(b) Measured ϕ/L(°/cm)	Error in ϕ/L(°/cm)
360	2.35	0.05	2.17	0.23
180	2.24	0.16	2.17	0.23
90	2.27	0.13	1.95	0.43

TABLE V. Measurement of phase shift as a function of path length change (ϕ/L) in air using the 140 MHz PMD and APD at 786 nm when (a) only the 786 nm laser diode is turned on and (b) both the 786 and 830 nm laser diodes are turned on, at different signal to noise ratios (measurement bandwidth is 10 Hz). At each signal to noise ratio, the signal output from the APD for both laser diodes was equivalent.

Signal to noise	(a) ϕ/L(°/cm)	(a) Error in ϕ/L(°/cm)	(b) ϕ/L(°/cm)	(b) Error in ϕ/L(°/cm)
2120	1.81	0.12	1.93	0.25
1420	1.90	0.22	1.98	0.30
950	2.10	0.42	2.22	0.62

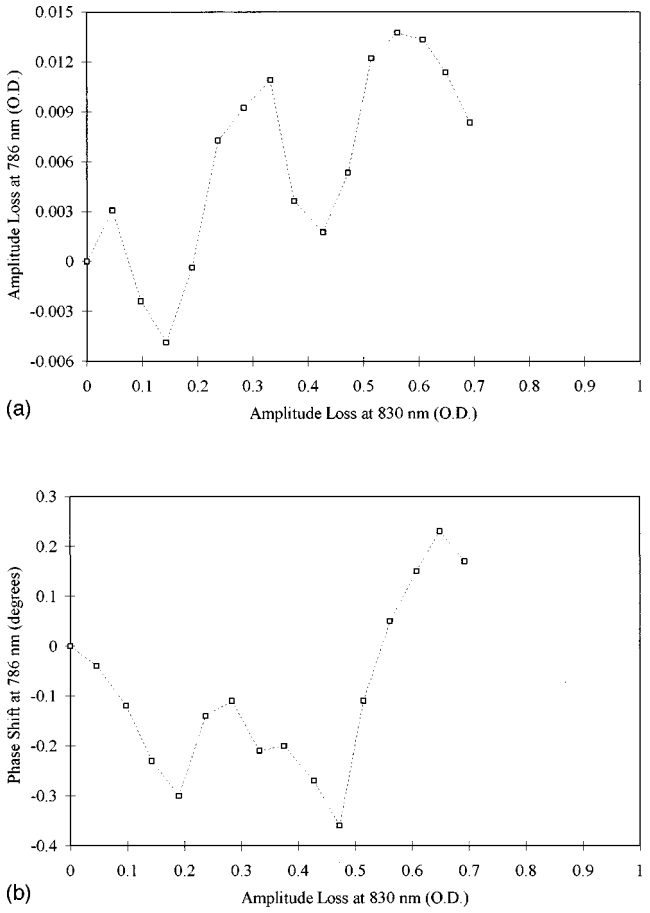

FIG. 14. (a) Amplitude loss measured from the 786 nm signal due to a 1.0 O.D. loss of the 830 nm wavelength source; (b) phase shift of the 786 nm signal due to a 1.0 O.D. amplitude loss of the 830 nm laser source. Measurements were made in a 10 Hz bandwidth.

could potentially cause a significant error in the measurement of phase shifts in tissue. Software correction of the phase shift due to amplitude attenuation is cumbersome, especially for the case in which the PMT is used due to the fact that the phase shift is a function of both the photocurrent and gain in the optical detector. Dynode feedback offers a solution to the phase-amplitude crosstalk. By maintaining a constant amplitude at the output of the PMT, the phase shift due to amplitude attenuation in the optical detector is minimized. Although there is a phase shift due to a change in the high voltage (electron multiplication), this is a reproducible quantity which is related linearly to the high voltage and can be easily corrected in software.

Finally, a comparison of the phase errors due to interchannel interference resulting from frequency and time multiplexing indicate that with time multiplexing, the phase errors are significantly lower. Although the inherent advantage of frequency multiplexing is that multiwavelength measurements can be performed simultaneously enabling the use of this technique in wide band measurements, the results of our study show that there are several issues that need to be considered in developing a frequency encoded multiwavelength PMD. Appropriate offset radio frequencies for modulation of the laser sources at the different wavelengths must be selected such that intermodulation products are minimized and the rf source has to have a low harmonic content. Both these issues can render the development of a frequency encoded multiwavelength PMD complex and expensive. Although, multiwavelength operation must be implemented serially in the time encoded PMD, it is a feasible alternative due to the fact that optical signals measured from tissue generally have a low bandwidth (1–10 Hz). Implementation of time multiplexing can be done electronically through the use of an electromechanical switch between the rf source and the multiple laser diodes enabling serial modulation of each wavelength source. Another advantage of the time multiplexed PMD is that one transmitter/receiver can be used instead of replicate transmitter/receiver pairs which simplifies the complexity and cost of the PMD.

[1] B. C. Wilson, in *Encyclopedia of Human Biology* (Academic, New York, 1991), Vol. 5.
[2] B. Chance, in *Oxygen Transport to Tissue XV*, edited by P. Vaupel (Plenum, New York, 1994).
[3] C. S. Robertson, S. P. Gopinath, and B. Chance, J. Neurotrauma **12**, 591 (1995).
[4] S. P. Gopinath, C. S. Robertson, C. F. Contant, R. K. Narayan, R. G. Grossman, and B. Chance, J. Neurosurg. **83**, 438 (1995).
[5] F. F. Jobsis-Vandervliet, in *Fetal and Neonatal Physiological Measurements*, edited by H. N. Lafeber (Elsevier Science, Netherlands, 1991).
[6] B. Beauvoit, S. M. Evans, T. W. Jenkins, E. E. Miller, and B. Chance, Anal. Biochem. **226**, 167 (1995).
[7] J. S. Maier, S. A. Walker, S. Fantini, M. A. Francheschini, and E. Gratton, Opt. Lett. **19**, 2062 (1994).
[8] H. Liu, B. Beauvoit, M. Kimura, and B. Chance, J. Biomed. Opt. **1**, 200 (1996).
[9] A. Ishimaru, Appl. Opt. **28**, 2210 (1989).
[10] I. D. Campbell and A. D. Raymond, *Biological Spectroscopy* (Benjamin/Cummings, Menlo Park, CA, 1984).
[11] B. C. Wilson, E. M. Sevick, M. S. Patterson, and B. Chance, Proc. IEEE **80**, 918 (1992).
[12] B. Chance, M. Cope, E. Gratton, N. Ramanujam, and B. Tromberg, Rev. Sci. Instrum. (in press).
[13] M. S. Patterson, B. Chance, and B. C. Wilson, Appl. Opt. **28**, 2331 (1989).
[14] J. B. Fishkin and E. Gratton, J. Opt. Soc. Am. **10**, 127 (1993).
[15] E. M. Sevick, B. Chance, J. Leigh, S. Nioka, and M. Maris, Anal. Chem. **195**, 330 (1991).
[16] S. Fantini, M. A. Franchesini-Fantini, J. S. Maier, S. A. Walker, B. Barbieri, and E. Gratton, Opt. Eng. (Bellingham) **34**, 32 (1995).
[17] S. Yokoyama, A. Okamoto, T. Araki, and N. Suzuki, Rev. Sci. Instrum. **66**, 5331 (1995).
[18] B. W. Pogue and M. S. Patterson, J. Biomed. Opt. **1**, 311 (1996).
[19] Y. Yang, H. Liu, X. Li, and B. Chance, Opt. Eng. **36**, 1562 (1997).
[20] T. Araki, Rev. Sci. Instrum. **66**, 43 (1995).